

# X-ray Radiation Induces Deprotonation of the Bilin Chromophore in Crystalline *D. radiodurans* Phytochrome

Feifei Li,<sup>†,‡</sup> E. Sethe Burgie,<sup>‡</sup> Tao Yu,<sup>\*,§</sup> Annie Héroux,<sup>†</sup> George C. Schatz,<sup>§</sup> Richard D. Vierstra,<sup>\*,‡</sup> and Allen M. Orville<sup>\*,†,||</sup>

<sup>†</sup>Photon Sciences Directorate and <sup>||</sup>Biosciences Department, Brookhaven National Laboratory, Upton, New York 11973, United States

<sup>‡</sup>Department of Genetics, the University of Wisconsin-Madison, Madison, Wisconsin 53706, United States

<sup>§</sup>Department of Chemistry, Northwestern University, Evanston, Illinois 60208, United States

<sup>#</sup>Department of Chemistry and Biochemistry, New Mexico State University, Las Cruces, New Mexico 88011, United States

**S** Supporting Information

**ABSTRACT:** We report that in the red light-absorbing (Pr) state, the bilin chromophore of the *Deinococcus radiodurans* proteobacterial phytochrome (DrBphP) is hypersensitive to X-ray photons used in typical synchrotron X-ray protein crystallography experiments. This causes the otherwise fully protonated chromophore to deprotonate without additional major structural changes. These results have major implications for our understanding of the structural and chemical characteristics of the resting and intermediate states of phytochromes and other photoreceptor proteins.

Phytochromes (Phys) are proteinaceous photoreceptors that play an integral role in nearly all aspects of plant photomorphogenesis.<sup>1,2</sup> Thus, understanding their structural, physical, and chemical characteristics is of great importance to appreciate how they function in plant physiology, and, by extension, how plants respond to light stimuli to optimize their growth and reproduction in their ever-changing light environment.<sup>3–7</sup> Photointerconversion of Phys between red and far-red light-absorbing forms ( $P_r$  and  $P_{fr}$ , respectively) is accomplished by virtue of a bilin chromophore, an open-chained tetrapyrrole.<sup>3–7</sup> Absorption of light typically induces photoisomerization of the C15=C16 double bond found between the C and D pyrrole rings with an associated  $\sim 180^\circ$  rotation of the D pyrrole ring (Scheme 1). The resulting Z to E flip proceeds via a series of spectroscopically observed intermediates (e.g., Lumi and Meta states) for the photoisomerization from the  $P_r$  to the  $P_{fr}$  state.<sup>4</sup> The photosensory module of canonical Phys comprises sequential Per/Arnt/Sim (PAS), cGMP-phosphodiesterase/

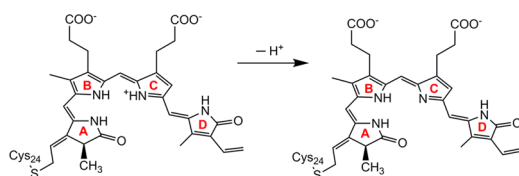
adenylyl cyclase/FhlA (GAF), and phytochrome-specific (PHY) domains.<sup>3–7</sup> The bilin chromophore is bound deeply within the GAF domain; both PAS and PHY domains are also important for proper photochemistry to occur, with the PHY domain stabilizing the photoactivated  $P_{fr}$  state.<sup>3–7</sup>

The discovery of Phys in bacteria and their subsequent structural characterization by X-ray crystallography were major steps toward understanding plant Phys.<sup>8</sup> The first high resolution structures were derived from the PAS-GAF region in the  $P_r$  state, which was obtained from the proteobacterial Phy (BphP) of *Deinococcus radiodurans* (DrBphP) assembled with its native biliverdin IX $\alpha$  (BV) chromophore using the PAS-GAF moiety.<sup>9,10</sup> While there was some suspicion of radiation sensitivity of the incorporated bilin in this and subsequent structural studies,<sup>10–14</sup> there has yet to be a clear understanding in this regard. Given the importance of X-ray crystallography in characterizing the structures of Phys and other photoreceptors,<sup>9,11–23</sup> assessing the underpinnings of chromophore sensitivity is urgently needed so we can infer the applicability of current Phy structures to the conclusions that have been drawn. Herein, we report that the bilin chromophore of DrBphP in the Pr state is hypersensitive to X-ray exposure, and readily deprotonates.

During our structural reinvestigation of the PAS-GAF domain region from DrBphP using X-ray crystallography, we observed a discoloration of the DrBphP crystal after exposing the crystal to synchrotron X-ray photons at 100 K (Figure 1A Inset). The crystal color changed from light greenish yellow to a much darker color; this color change was noticeable after only a few frames of a routine X-ray diffraction experiment. In a control experiment, we did not observe changes in either the color or the absorption spectrum of the cryo-buffer (SI Figure S1). This indicates that the electronic structure of the DrBphP chromophore changes upon exposure to X-ray radiation, which may parallel structural changes of this moiety.

To shed further light on the possible X-ray induced structural changes of DrBphP, it is critical to correlate high resolution electron density maps with spectroscopic changes and accumulated X-ray dose. The plate-like morphology and the

**Scheme 1. X-ray Radiation Deprotonates the Bilin Chromophore of a Bacteriophytochrome in the Pr State**



Received: October 23, 2014

Published: February 4, 2015

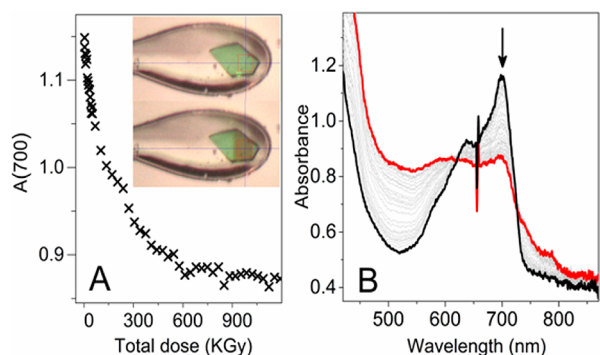


**Figure 1.** Single crystal UV–vis spectra of the PAS-GAF fragment from *Deinococcus radiodurans* BphP assembled with BV as a function of X-ray exposure at 100 K. Panel A: The change in absorbance at 700 nm of a single crystal of DrBphP as a function of accumulated X-ray dose. Panel A inset: beamline camera views of a DrBphP crystal before (top) and after (bottom) after 500 KGy accumulated X-ray dose (red box indicates a  $100 \times 100 \mu\text{m}^2$  X-ray beam centered at the blue crosshair). Panel B: Single crystal diode-array UV–vis spectra of DrBphP at 100 K as the accumulated X-ray dose increased from 0 (black line) to 500 KGy (red line). See SI Figure S3 for difference spectra.

very well diffracting characteristics of the DrBphP(PAS-GAF) crystals are ideal for creating correlated composite data sets by merging dose-controlled data from several crystals. To determine the cutoff dose required for a low-dose electron map, we followed the X-ray dose dependence of the single crystal UV–vis absorbance at 700 nm, the  $\lambda_{\text{max}}$  of the signature band characteristic of the Pr state of DrBphP (Figure 1A). Interestingly, there was a noticeable decrease of  $A(700)$  after the very first frame (ca. 1–3 KGy), suggesting that the perturbations of the DrBphP chromophore require very little dose. Indeed, approximately 100 KGy exposure was sufficient to introduce half of this spectroscopic change based on  $A(700)$ , which is well below the diffraction-quality-based radiation dose limit (30000 KGy) previously established for typical cryo-cooled protein crystals during X-ray structure determination.<sup>24</sup> With a mere accumulated X-ray dose of 15 KGy,  $A(700)$  decayed by ~5% (Figure 1A).

With the cutoff dose of 15 KGy selected for the low X-ray dose structure, we collected and merged X-ray diffraction frames on 130 non-overlapping regions of 11 DrBphP crystals. This allowed us to generate and refine 1.7 Å resolution electron density maps using controlled doses. As shown in Figure 2, Map A (top panel) was obtained with a very low accumulated X-ray dose of  $\leq 15$  KGy, and Map B (bottom panel) with an accumulated dose of 460–520 KGy (see SI Table S1 for data collection and refinement statistics). For these dose-controlled data sets, the refined structures were almost identical to the published Pr state structures 2O9C<sup>10</sup> and 4Q0H,<sup>21</sup> with root-mean-square (rms) deviations of 0.124 and 0.106, respectively, for the 319 C $\alpha$  atoms included in the 2O9C model. The BV conformation, including the positions and orientations of the A–D rings, was very similar in all these structures. The ZZZ<sub>ssa</sub> configuration was also retained with the torsion angle of 44° between the D ring and the plane consisting of the C and B rings, as in the published structures.<sup>10</sup> The well-ordered “pyrrole water” molecule and its hydrogen bonding to the pyrrole rings A–C were also observed in maps A and B. The B factor of the “pyrrole water” was comparable to the neighboring atoms of the pyrrole rings in all maps (11.14 for the low-dose structure, and 15.94 for the high-dose structure). The electron densities around the

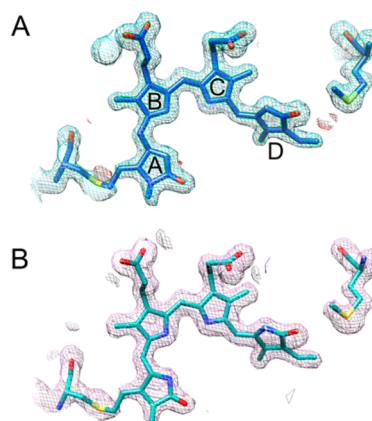


**Figure 2.** Comparison of the BV chromophore conformations as Pr in the three-dimensional X-ray crystal structures of the PAS-GAF fragment of DrBphP collected with a very low accumulated X-ray dose of  $\leq 15$  KGy (panel A) and a higher accumulated X-ray dose of 460–520 KGy (panel B) at 100 K. 2Fo–Fc electron density maps (blue for A and purple for B) were calculated to 1.7 Å resolution. Fo–Fc maps are shown in red (negative) and green (positive). Contour levels are  $1\sigma$  for 2Fo–Fc maps and  $\pm 3\sigma$  for Fo–Fc maps.

thioether linkage connecting the C3<sup>2</sup> carbon of BV to Cys-24 were highly similar between maps A and B, with the thioether bond analogously maintained.<sup>25</sup> Overall, the refined structures do not reveal any major structural rearrangements of either the protein residues or the bilin chromophore.

To better define the nature of the X-ray induced reactions occurring within DrBphP crystals, we studied the time-resolved diode-array single crystal UV–vis absorption spectra of DrBphP-(PAS-GAF) correlated with the X-ray diffraction study at 100 K (see Supporting Information (SI) for experimental details). As shown in Figure 1B, the single crystal absorption spectrum of a fresh DrBphP crystal featured a  $\lambda_{\text{max}}$  at 700 nm characteristic of the Q-band of the DrBphP Pr state with a protonated bilin. This feature gradually decayed with an increasing X-ray dosage, which was accompanied by the evolution of a shoulder-like band at ~750 nm and a broad absorption feature between 420 and 600 nm (Figure 1B and SI Figure S2). The Q-band was established as the HOMO to LUMO transition of the chromophore based on previous TD-DFT studies.<sup>26</sup> The decreased oscillator strength of the signature Q bands suggested that BV became deprotonated.<sup>27,28</sup> Such decreased Q-band intensity as a result of chromophore deprotonation was previously reported in the pH-dependence of the Agp2 BphP Pr state.<sup>27</sup> This is also very reminiscent of the UV–vis spectrum of a deprotonated intermediate, Meta-R<sub>c</sub> of Agp1 BphP that was obtained by cryogenic trapping.<sup>28</sup>

Another piece of evidence supporting the deprotonation of BV came from single crystal Raman studies. Using a 473 nm laser excitation to probe the preresonance region, a fresh DrBphP-(PAS-GAF) crystal in the Pr state exhibited the signature 1624  $\text{cm}^{-1}$  band assigned to the C15=C16 stretching of the C–D ring methine bridge (Figure 3). This 1624  $\text{cm}^{-1}$  band represents the strongest peak in the so-called “marker band region” (1500–1700  $\text{cm}^{-1}$ ),<sup>29</sup> which was also the case in the reported spectra of DrBphP(PAS-GAF) collected with a 1064 nm laser.<sup>30</sup> The stretching mode of the A–B ring methine bridge C5=C6 is observed at 1648  $\text{cm}^{-1}$  as a second signature peak. Other than the C=C stretching modes, the presence or absence of the N–H in-plane (*ip*) bending modes of the B and C rings between 1550

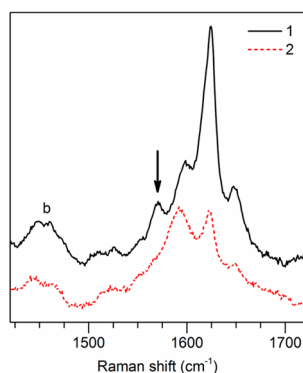


**Figure 3.** Single crystal Raman spectra of DrBphP(PAS-GAF) as Pr taken prior to (1, black solid line) and after (2, red dashed line) exposing the crystal to >400 KGy X-ray dose that causes the full decay of A(700). Black arrow denotes the N—H in-plane (*ip*) bending mode at 1571  $\text{cm}^{-1}$ . Data collection conditions: 100 K, 473 nm laser, 4.8 mW. b = cryo-buffers.

and 1580  $\text{cm}^{-1}$  has been well established as a marker band for the protonation state of the BphP chromophore.<sup>31</sup> Here, the N—H *ip* bending mode of B and C rings of DrBphP manifested at 1571  $\text{cm}^{-1}$ ; upon D<sub>2</sub>O labeling, this band disappeared (SI Figure S4). The existence of this band and the effectiveness of H/D exchange were consistent with a cationic protonated BV in fresh crystals of DrBphP, with the protonation of the bilin in agreement with a recent 1.16 Å structure of DrBphP(PAS-GAF).<sup>21</sup>

After the X-ray-induced deprotonation of DrBphP was completed as indicated by the single crystal UV–vis spectra, the resonance Raman spectra of the crystal were collected and compared to those acquired before any X-ray exposure. The two strongest peaks shifted to 1592 and 1623  $\text{cm}^{-1}$  (Figure 3), respectively, corresponding to the C=C stretching mode of the C–D and A–B ring methine bridge, respectively. These downshifts in Raman frequencies of C=C methine bridges were reminiscent of those observed when transforming the Pr state into the B/C-ring deprotonated Meta-R<sub>c</sub> state<sup>32</sup> of Agp1 in solution.<sup>28</sup> In addition, the 1571  $\text{cm}^{-1}$  peak from the N—H *ip* bending mode disappeared (Figure 3), and there were no prominent bands from 1500 to 1590  $\text{cm}^{-1}$ , the marker region for the BV protonation state. The disappearance of the N—H *ip* bending modes indicated a loss of proton(s) from the cationic pyrrole rings of DrBphP. A loss of the N—H *ip* modes was similarly observed in the Meta-R<sub>c</sub> state with the B/C ring deprotonated.<sup>28</sup>

To lend further credence to the notion of the bilin chromophore deprotonation, we carried out molecular dynamics (MD) simulation of the BV bound to DrBphP to investigate whether there has to be a major conformational change of the chromophore to accommodate the deprotonation (see SI for simulation details). As shown in Figure 4, the overall orientations of the pyrrole rings deprotonated at either the C ring (red) or the B ring (orange) were very analogous to those of the cationic protonated bilin (blue). The simulation results agree with our experimental data and suggest that the chromophore-binding pocket of DrBphP can encompass the deprotonated form of BV without forcing additional major structural changes in the binding crevice.

To summarize, we demonstrate that the bilin cofactor of the phytochrome photoreceptor proteins is hypersensitive to X-ray photons, even under cryogenic conditions. We further show that exposure to X-ray photons causes the bilin chromophore within

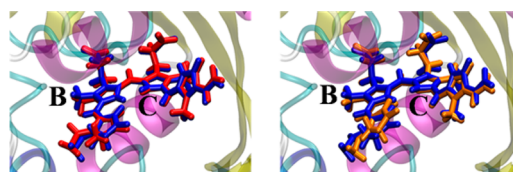


**Figure 4.** Molecular dynamics simulations to optimize the structures of the C-ring deprotonated (red, left) and the B-ring deprotonated (orange, right) tetrapyrrole active site, in relationship to the fully protonated (blue) tetrapyrrole active site at 100 K.

the DrBphP(PAS-GAF) crystal in the Pr state to deprotonate without the BV isomerizing or undergoing other major structural changes.<sup>33</sup> This process was half-completed with ~100 KGy accumulated X-ray dose. While a recommended dose limit for global changes of proteins in a typical macromolecular crystallography experiment is 30 000 KGy,<sup>24</sup> our results demonstrate that the specific modification of the bilin (i.e., the deprotonation process) of DrBphP is 2 orders of magnitude more sensitive to X-ray exposure. Our conclusions are bolstered by a combination of X-ray crystallography, single crystal UV–vis studies correlated with X-ray diffraction, single crystal Raman spectroscopy, and MD simulations.

While radiation sensitivity of BphP has been cautioned previously,<sup>10–14</sup> a systematic experimental approach to pinpoint which and how specific chemical functionalities are modified has not heretofore been conducted. The level of detail presented in our work fills this gap of knowledge. For comparison, X-ray-induced photoreduction of iron centers coordinated by cyclic tetrapyrrole cofactors in heme enzymes was reported by some of the authors here<sup>34</sup> and others.<sup>35,36</sup> Without a tetrapyrrole-bonded metal center, deprotonation of the linearized bilin is observed in our study, with the “pyrrole water” hydrogen-bonded to rings A–C presumably mediating the proton transfer process. After a rapid light-induced isomerization of the bilin chromophore, light-induced deprotonation followed by reprotonation is thought to comprise the central step of the photoconversion of Phys from P<sub>r</sub> to P<sub>f</sub>; this process is stalled in a deprotonated Meta-R<sub>c</sub> intermediate for DrBphP PAS-GAF.<sup>30</sup> Herein, our detection of the sensitive X-ray-induced deprotonation without photoisomerization for the PAS-GAF fragment is not likely part of the normal photoconversion cycle. On the other hand, we cannot rule out the intriguing possibility that Phys have specifically evolved a sensitivity to ionizing radiation and use this subsequent deprotonation step as a heretofore unknown signal.<sup>37</sup>

Our findings have major implications for the fundamental understanding of the structural and chemical properties of phytochrome and also for the interaction of X-ray radiation with proteins in general. In view of our findings, the first high-resolution structure of DrBphP(PAS-GAF) previously reported “captured” the deprotonated state rather than the fully protonated Pr state.<sup>10</sup> It follows that X-ray induced structural changes of Phys in both resting and intermediate states are much more facile and ubiquitous than the scientific community has expected. Thus, the application of single crystal spectroscopy measurements correlated with X-ray diffraction experiments<sup>38,39</sup> has the potential to shift the paradigms of structural and reactivity studies into the superfamily of phytochromes and other photoreceptor proteins. In this vein, Anders et al. reported an X-ray induced intermediate state of a cyanobacterial phytochrome based on altered single crystal UV–vis spectra but could only infer the identity of the intermediate.<sup>14</sup> Herein, our studies

provide solid evidence to the deprotonated nature of the X-ray generated intermediate state of DrBpHP in crystallo. This will further inspire the generation and characterization of otherwise elusive metastable intermediate states relevant to the photo-induced isomerization of phytochromes and other photo-receptor proteins by leveraging the interactions of the bilin chromophore with X-ray photons.

## ■ ASSOCIATED CONTENT

### ● Supporting Information

Experimental details, Table S1, and Figure S1–S4. This material is available free of charge via the Internet at <http://pubs.acs.org>. Structure factors and coordinates have been deposited to the Protein Data Bank with reference codes 4Y3I and 4Y5F for the low-dose and higher-dose structures, respectively.

## ■ AUTHOR INFORMATION

### Corresponding Authors

\*tao.yu1@northwestern.edu.

\*vierstra@wisc.edu.

\*amorv@bnl.gov.

### Notes

The authors declare no competing financial interest.

## ■ ACKNOWLEDGMENTS

We thank Dr. Babak Andi for helpful discussions, and Dr. Maria A. Mroginski for kindly sending the force field parameters. F.L., A.H., and A.M.O. were supported by NIH/NIGMS grant 8P41GM103473-16, and DOE/BER grant FWP BO-70. E.S.B. and R.D.V. were supported by the NSF grant MCB-1329956. T.Y. and G.C.S. acknowledge support from the Ultrafast Initiative of the U. S. Department of Energy, Office of Science, Office of Basic Energy Sciences, through Argonne National Laboratory under Contract No. DE-AC02-06CH11357. Data were collected at beamlines X26-C and X25 of the National Synchrotron Light Source (NSLS), which was supported under Contract No. DE-AC02-98CH10886 of U.S. Department of Energy Office of Basic Energy Sciences.

## ■ REFERENCES

- (1) Briggs, W. R.; Spudich, J. L. *Handbook of Photosensory Receptor*; Wiley: Weinheim, 2005.
- (2) Franklin, K. A.; Quail, P. H. *J. Exp. Bot.* **2010**, *61*, 11.
- (3) Rockwell, N. C.; Lagarias, J. C. *Plant Cell* **2006**, *18*, 4.
- (4) Mroginski, M. A.; Murgida, D. H.; Hildebrandt, P. *Acc. Chem. Res.* **2007**, *40*, 258.
- (5) Nagatani, A. *Curr. Opin. Plant Biol.* **2010**, *13*, 565.
- (6) Hughes, J. *Biochem. Soc. Trans.* **2010**, *38*, 710.
- (7) Ulijasz, A. T.; Vierstra, R. D. *Curr. Opin. Plant Biol.* **2011**, *14*, 498.
- (8) Burgie, E. S.; Bussell, A. N.; Walker, J. M.; Dubiel, K.; Vierstra, R. D. *Proc. Natl. Acad. Sci. U. S. A.* **2014**, *111*, 10179.
- (9) Wagner, J. R.; Brunzelle, J. S.; Forest, K. T.; Vierstra, R. D. *Nature* **2005**, *438*, 325.
- (10) Wagner, J. R.; Zhang, J.; Brunzelle, J. S.; Vierstra, R. D.; Forest, K. T. *J. Biol. Chem.* **2007**, *282*, 12298.
- (11) Yang, X.; Stojkovic, E. A.; Kuk, J.; Moffat, K. *Proc. Natl. Acad. Sci. U. S. A.* **2007**, *104*, 12571.
- (12) Essen, L.-O.; Mailliet, J.; Hughes, J. *Proc. Natl. Acad. Sci. U. S. A.* **2008**, *105*, 14709.
- (13) Yang, X.; Ren, Z.; Kuk, J.; Moffat, K. *Nature* **2011**, *479*, 428.
- (14) Anders, K.; Daminelli-Widany, G.; Mroginski, M. A.; von Stetten, D.; Essen, L.-O. *J. Biol. Chem.* **2013**, *288*, 35714.
- (15) Yang, X.; Kuk, J.; Moffat, K. *Proc. Natl. Acad. Sci. U. S. A.* **2008**, *105*, 14715.
- (16) Ulijasz, A. T.; Cornilescu, G.; Cornilescu, C. C.; Zhang, J.; Rivera, M.; Markley, J. L.; Vierstra, R. D. *Nature* **2010**, *463*, 250.
- (17) Narikawa, R.; Ishizuka, T.; Muraki, N.; Shiba, T.; Kurisu, G.; Ikeuchi, M. *Proc. Natl. Acad. Sci. U. S. A.* **2012**, *110*, 918.
- (18) Salewski, J.; Escobar, F. V.; Kaminski, S.; von Stetten, D.; Keidel, A.; Rippers, Y.; Michael, N.; Scheerer, P.; Piwowarski, P.; Bartl, F.; Frankenberg-Dinkel, N.; Ringsdorf, S.; Gärtner, W.; Lamparter, T.; Mroginski, M. A.; Hildebrandt, P. *J. Biol. Chem.* **2013**, *288*, 16800.
- (19) Rockwell, N. C.; Ohlendorf, R.; Möglich, A. *Proc. Natl. Acad. Sci. U. S. A.* **2013**, *110*, 806.
- (20) Burgie, E. S.; Walker, J. M.; Phillips, G. N.; Vierstra, R. D. *Structure* **2013**, *21*, 88.
- (21) Burgie, E. S.; Wang, T.; Bussell, A. N.; Walker, J. M.; Li, H.; Vierstra, R. D. *J. Biol. Chem.* **2014**, *289*, 24574.
- (22) Cornilescu, C. C.; Cornilescu, G.; Burgie, E. S.; Markley, J. L.; Ulijasz, A. T.; Vierstra, R. D. *J. Biol. Chem.* **2014**, *289*, 3055.
- (23) Takala, H.; Björling, A.; Berntsson, O.; Lehtivuori, H.; Niebling, S.; Hoerlne, M.; Kosheleva, I.; Henning, R.; Menzel, A.; Ihalainen, J. a; Westenhoff, S. *Nature* **2014**, *509*, 245.
- (24) Owen, R. L.; Rudiño-Piñera, E.; Garman, E. F. *Proc. Natl. Acad. Sci. U. S. A.* **2006**, *103*, 4912.
- (25) While it was hypothesized that the thioether linkage might be very sensitive to X-ray exposure,<sup>10–14</sup> we did not observe any significantly different electron densities in this region between map A and map B.
- (26) Matute, R. A.; Contreras, R.; González, L. *J. Phys. Chem. Lett.* **2010**, *1*, 796.
- (27) Zienicke, B.; Molina, I.; Glenz, R.; Singer, P.; Ehmer, D.; Escobar, F. V.; Hildebrandt, P.; Diller, R.; Lamparter, T. *J. Biol. Chem.* **2013**, *288*, 31738.
- (28) Borucki, B.; Von Stetten, D.; Seibeck, S.; Lamparter, T.; Michael, N.; Mroginski, M. A.; Otto, H.; Murgida, D. H.; Heyn, M. P.; Hildebrandt, P. *J. Biol. Chem.* **2005**, *280*, 34358.
- (29) Von Stetten, D. *Investigation of the chromophore structure in plant and bacterial phytochromes by comparison of experimental and calculated Raman spectra*; Ph.D. Dissertation, Technische Universität Berlin, 2008.
- (30) Von Stetten, D.; Günther, M.; Scheerer, P.; Murgida, D. H.; Mroginski, M. A.; Krauss, N.; Lamparter, T.; Zhang, J.; Anstrom, D. M.; Vierstra, R. D.; Forest, K. T.; Hildebrandt, P. *Angew. Chem., Int. Ed.* **2008**, *47*, 4753.
- (31) Mroginski, M. A.; von Stetten, D.; Escobar, F. V.; Strauss, H. M.; Kaminski, S.; Scheerer, P.; Günther, M.; Murgida, D. H.; Schmieder, P.; Bongards, C.; Gärtner, W.; Mailliet, J.; Hughes, J.; Essen, L.-O.; Hildebrandt, P. *Biophys. J.* **2009**, *96*, 4153.
- (32) We remind readers that there are no characteristic vibrational bands in Raman spectra that pinpoint a deprotonated chromophore in the ZZE (as in the Meta-R<sub>c</sub> form) vs ZZZ configuration (as in this work).
- (33) The BV deprotonation upon X-ray exposure is expected to proceed similarly for Phys equipped with a full photosensory module, as the PAS-GAF domains in recent crystal structures<sup>21,23</sup> of the DrBpHP (PAS-GAF-PHY) superimpose remarkably well with those of PAS-GAF fragments alone.
- (34) Yi, J.; Orville, A. M.; Skinner, J. M.; Skinner, M. J.; Richter-Addo, G. B. *Biochemistry* **2010**, *49*, 5969.
- (35) Hersleth, H.-P.; Andersson, K. K. *Biochim. Biophys. Acta* **2011**, *1814*, 785.
- (36) Meharena, Y. T.; Doukov, T.; Li, H.; Soltis, S. M.; Poulos, T. L. *Biochemistry* **2010**, *49*, 2984.
- (37) Makarova, K. S.; Aravind, L.; Wolf, Y. I.; Tatusov, R. L.; Minton, K. W.; Koonin, E. V.; Daly, M. J. *Microbiol. Mol. Biol. Rev.* **2001**, *65*, 44.
- (38) Owen, R. L.; Yorke, B. A.; Gowdy, J. A.; Pearson, A. R. *J. Synchrotron Radiat.* **2011**, *18*, 367.
- (39) Orville, A. M.; Buono, R.; Cowan, M.; Héroux, A.; Shea-McCarthy, G.; Schneider, D. K.; Skinner, J. M.; Skinner, M. J.; Stoner-Ma, D.; Sweet, R. M. *J. Synchrotron Radiat.* **2011**, *18*, 358.